Journal of Thermal Analysis and Calorimetry, Vol. 55 (1999) 569-579

Measurement of sorption, chemical and physical reactions

GRAVIMETRIC STUDY OF INTERACTION OF WATER VAPOUR WITH METALLIC ZINC

J. C. Bazán, M. E. Gschaider and G. A. Alimenti

Departamento de Química e Ingeniería Química, Universidad Nacional del Sur
8000 Bahía Blanca, Argentina

Abstract

The interaction between samples of metallic zinc and water vapour was studied gravimetrically, both in the absence and in the presence of oxygen. The experimental total mass gain *vs.* time curves exhibited two plateaus, whose heights increased with, elevations both of relative humidity and of temperature. The amount of product retained on the surface after desorption was also determined as a function of time. The product was identified as hydrated zinc oxide. In the runs conducted without oxygen, the retained product curves displayed a time delay with respect to the total mass gain curves. In the presence of oxygen, however, there was practically only one chronogravimetric curve. This behaviour is interpreted on the basis of a common mechanism involving the formation of an intermediate precursor oxide, which is more readily formed in the presence of oxygen than in its absence. A set of mathematical equations was derived, from which the rate constants for both processes were obtained. The second step was ascribed to a further weak adsorption of water.

Keywords: gravimetry, hydrated zinc oxide, metallic zinc, water vapour

Introduction

A systematic study of chemical reactions between solid electrolytes and metals revealed that the presence of water vapour is fundamental for the process, as found for instance in a previous work on the reaction between aluminum and silver iodide [1]. Similarly, it was found that the reaction of silver iodide and zinc depends markedly on the presence of water vapour [2]. Although the reaction of water with zinc to give hydrated zinc oxide is well known as a fundamental step in the corrosion of zinc in contact with either aqueous solutions or humid atmospheres [3], as far as the present authors are aware, there has been no systematic study on the influence of water vapour pressure or relative humidity (*RH*) on this

1418–2874/99/ $ 5.00

Akadémiai Kiadó, Budapest
Kluwer Academic Publishers, Dordrecht

process. Thus, as a contribution to this subject, the present communication deals with the interaction of metallic zinc with humid atmospheres both in the presence and in the absence of oxygen.

Experimental

The process was followed by recording the mass gain of chemically polished zinc discs of 99.99% purity, about 1 cm in diameter and 0.05 cm thick, in contact with atmospheres with *RH* between 0.30 and 0.95. The temperature range was between 21 and 50°C. Water vapour atmosphere of well-defined *RH* [4], in which oxygen was present at atmospheric partial pressure was obtained with saturated aqueous inorganic solutions. When no oxygen was desired in the runs, it was eliminated by evacuation to about 0.01 mm Hg (1.33 Pa), followed by equilibration to atmospheric pressure by injection of 99.99% pure nitrogen. In this way, the oxygen content in the reaction chamber was lower than 0.01%, as determined by gas chromatographic analysis. Some runs were also conducted with dried air, i.e. at zero *RH*.

The measurements were carried out with a Cahn 1000 Vacuum Recording Electrobalance, in which the weighing chamber was attached to the hangdown tube and connected to a vacuum line and to a humidity source through vacuum stopcocks. The sample disc was suspended vertically from a special holder, in order to expose both faces. A similar holder was attached to the other arm of the balance, and the starting zero-point was reached by means of the balance controls. No buoyancy effects were detected in work at around room temperature. In the measurements at 30°C and higher, however, it was necessary to ensure a similar temperature in both arms in order to eliminate buoyancy.

Preliminary runs demonstrated that the mass gain involves two contributions: a strongly retained portion and a readily desorbed portion; accordingly, two types of recording were made. In the first, the continuous total mass gain (m) as a function of time to constant mass was registered. At the end of the runs, the re-

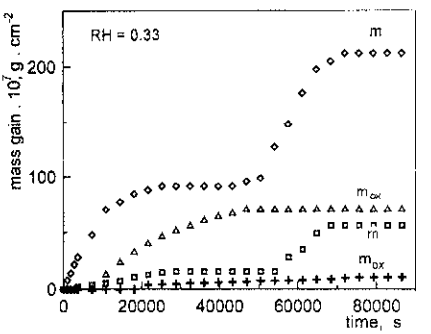

Fig. 1 Total mass (m) and mass of product (m_{ox}) *vs.* time curves; + – 21°C, □ – 21°C, △ – 42°C, ◊ – 42°C

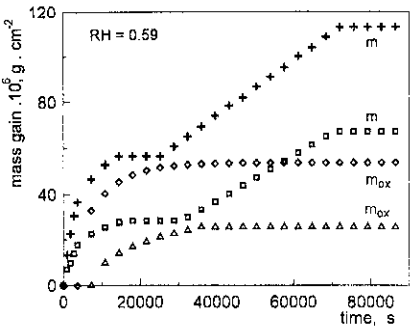

Fig. 2 Total mass (m) and mass of product (m_{ox}) *vs.* time curves; ▵ – 42°C, □– 42°C, + – 50°C, ◊ – 50°C

action chamber was evacuated at about 0.01 mm Hg and the mass of reaction product retained on the metal sample (m^0_{ox}) was determined.

In the second type of measurement, the mass retained after evacuation for different reaction times was determined (m_{ox}). In this way, the amount of product was obtained as a function of time.

As a rule, the samples reached constant mass after about 24 h.

The nature of the reaction product was established by means of both ESCA-XPS and GI-XRD. The morphology of the surface was studied by means of SEM-EDAX. These studies were made on samples reacted at the highest temperature and *RH*, in order to obtain a sufficient amount of reaction product. In work with samples consisting of several pieces of zinc, it was also established that the reaction involves the evolution of molecular hydrogen, as determined by gas chromatography.

Results and discussion

Mass gain recordings

Measurements without oxygen

Figures 1–3 depict typical examples of total mass gain (m) and retained mass (m_{ox}) as a function of time. Two steps are clearly defined for the former, whereas for the second only one is to be seen, with a plateau whose value (m^0_{ox}) is the closer to that of the first step (m_o), the higher the temperature. Coincidentally, determination of the mass retained by desorption after the second step of the total mass curves yields practically the same values as the plateau in the m_{ox} *vs.* time curves. It is also to be noted that the m_{ox} *vs.* time curves exhibit noteworthy values only after an induction period, which was the shorter, the higher the *RH* and/or the temperature. This points to the adsorption of a certain amount of water before the reaction starts. The plateau values increase with *RH* and temperature.

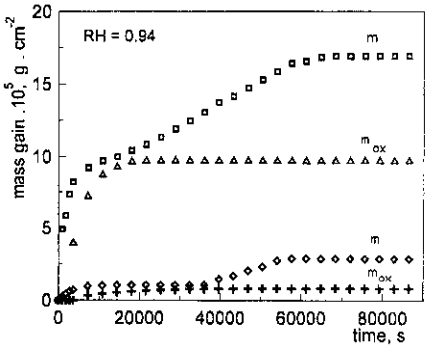

Fig. 3 Total mass (m) and mass of product (m_{ox}) *vs.* time curves; + – 21°C, ◊ – 21°C, △ – 50°C, □ – 50°C

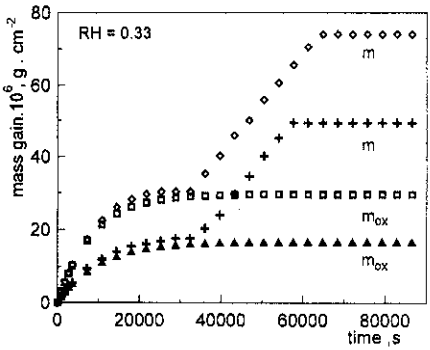

Fig. 4 Total mass (m) and mass of product (m_{ox}) *vs.* time curves; ▲ – 42°C,+ – 42°C, □– 50°C, ◊ – 50°C

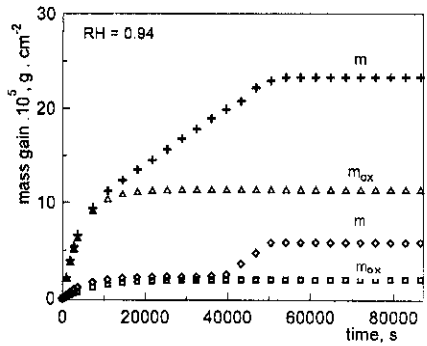

Fig. 5 Total mass (m) and mass of product (m_{ox}) *vs.* time curves; □ - 21°C, ◊ – 21°C, + – 42°C, △ – 42°C

Measurements in the presence of oxygen

Figures 4 and 5 present some typical curves of total mass (m) and retained mass (m_{ox}) as a function of time. As in the preceding case, two steps are to be observed. In this case, no induction period is to be seen; there is a clear coincidence between the total mass curves (m) and those of the amount retained after desorption (m_{ox}), except for the measurements carried out at 21°C. In this case too, the plateau values and the initial slopes increase with *RH* and temperature.

Morphology of the reacted surface

In all cases, SEM-EDAX observations revealed that the reaction does not form pits, but proceeds laterally. The product appears as small conglomerates whose size and distribution on the surface depend on the working conditions. Thus, at low *RH* and temperature, scarcely spread particles of about 0.5 to 10 μm are seen, whereas under more reactive conditions larger and more closely distributed conglomerates (about 20 μm) are found. As regards the nature of the reaction product, which was naturally expected to be ZnO, the EDAX determinations demonstrated only zinc and oxygen, in an atomic ratio very close to one. This was confirmed by GI-XRD measurements, in which only the lines corresponding to zinc oxide were found. XP spectroscopy determinations were also performed on samples reacted at high *RH* and temperature. In this case, as Zn and ZnO have very close binding energies which makes their differentiation difficult, the atomic ratio O/Zn was calculated, and proved to have a value higher than one. As this is generally ascribed to the presence of surface OH groups, it points to a residual layer of chemisorbed water. Thus, it is reasonable to conclude that the reaction product remaining after vacuum desorption is zinc oxide with some chemisorbed water, ZnO·nOH, as reported in the literature [5–7].

A comparison was made between the mass retained after desorption under the vacuum afforded by the mechanical pump and the mass of the average number of product particles counted by surface mapping of the same sample after SEM examination at 10^{-9} mm Hg. For a sample exposed to a *RH* of 94% at 21°C, the gravimetrically determined mass of the product was $1.20 \cdot 10^{-5}$ g, whereas that obtained by counting the surface particles was $1.1 \cdot 10^{-5}$ g; this is a noteworthy agreement, which may be fortuitous, but nevertheless supports the assumption made. In this calculation, the zinc oxide density was used, on the assumption that the surface OH groups would not appreciably change this.

Reaction mechanism

As mentioned above, it seems clear that, with or without the presence of oxygen, the reaction leads to hydrated zinc oxide, which in the presence of oxygen is formed in a single step, whereas without oxygen a previous adsorption process is needed before the reaction starts. As reported by Thiel and Madey [7], water dissociates when it interacts with a metallic surface, and more easily so when that

surface is to some extent covered with oxide or chemisorbed oxygen. In this way, the induction period found in the absence of oxygen could be explained as the time needed for the formation of a certain amount of what may be called 'precursor oxide' on the surface, upon which the reaction can be sustained. On the other hand, in the presence of oxygen, the reaction with water takes place directly, for it is reasonable to assume that in this case the necessary oxide centres are formed faster. On this basis, and bearing in mind the experimentally observed hydrogen evolution, the following mechanism schemes are proposed.

Without oxygen

1. physical water adsorption: $H_2O_{(v)} \rightleftarrows nH_2O_{(ad)}$
2. precursor oxide formation: $H_2O_{(ad)} + Zn_{(s)} \rightleftarrows Zn\cdots O + H_{2(g)}$
3. hydrated oxide formation:

$$Zn\cdots O + (n-1)H_2O_{(ad)} \rightarrow ZnO(n-1)\cdot OH + 1/2(n-1)\,H_{2(g)}$$

where n is not a stoichiometric factor, but the undefined number of water molecules adsorbed on the surface sites.

As concerns the second step in the total mass gain curves, it may be ascribed to a further weak adsorption of water on the formed oxide, for it is easily eliminated by the vacuum of the mechanical pump.

In the presence of oxygen

As mentioned above, no induction period (at least in the time scale of the present work) is observed, which may be explained in that the necessary precursor oxide is rapidly formed by the direct reaction of metallic zinc with oxygen. Thus, the postulated reaction scheme would be:

1. precursor oxide formation: $1/2O_{2(g)} + Zn_{(s)} \rightleftarrows Zn\cdots O$
2. hydrated oxide formation:

$$Zn\cdots O + n'H_2O_{(v)} \rightarrow ZnOn'OH + 1/2n'H_{2(g)}$$

Kinetic laws

In the absence of oxygen

Its seems evident that the reaction starts after the total mass gain has almost reached the first plateau, and ends when that amount has been completely converted into hydrated zinc oxide. This is suggested by the agreement between the mass at the first plateau (m_o) and the final mass of the retained product (m_{ox}). Furthermore, from the shape of the experimental curves, it is clear that the rate of the first adsorption process drops as time elapses, i.e. as the mass gain approaches the value for the first step. Thus, the adsorption process may be expressed by the following differential equation

$$\frac{d(m_{ads}/m_o)}{dt} = k_{ads}\left(1 - \frac{m_{ads}}{m_o}\right) \quad (1)$$

where m_{ads} is the mass of adsorbed water (the same as the total mass, m, during this stage), m_o is the mass in the first step, t is the reaction time, and k_{ads} is the rate constant for the adsorption process, which should be a function of RH and temperature. On integration:

$$\frac{m_{ads}}{m_o} = 1 - \exp(-k_{ads}\, t), \text{ or}$$
$$\ln(m_o - m_{ads}) = \ln m_o - k_{ads} t \quad (2)$$

Figures 6 and 7 present some plots of experimental data according to Eq. (2). From the straight lines obtained, the corresponding values of k_{ads} were obtained, which in turn are plotted as a function of RH in Fig. 8. From this graph, the dependences of k_{ads} on $(RH)^{2.2}$ at 21 and 33°C and on $(RH)^{1.3}$ at 42 and 52°C are obtained. It should be pointed out that the dependence found on RH pertains rather to the rate of reaction than to the reaction constant, as evident from Eq. (1).

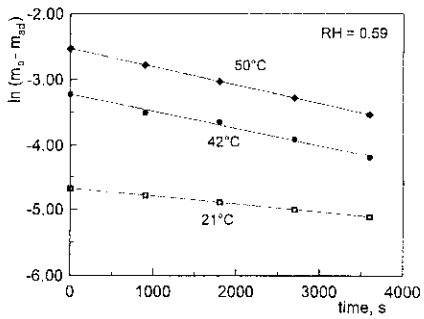

Fig. 6 Plots of experimental data as $\log(m_o - m_{ads})$ *vs.* time

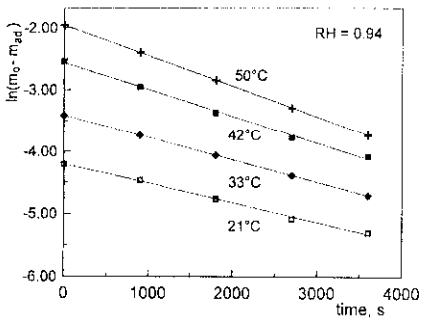

Fig. 7 Plots of experimental data as $\log(m_o - m_{ads})$ *vs.* time

Hence, these exponents may be associated with the value of n in the adsorption step of the reaction scheme. In this sense, the higher values obtained at 21 and 33°C may be assumed simply to reflect the fact that the extent of physisorption decreases with temperature. This explanation is also consistent with the fact that a comparison between the plateau values in the total mass *vs.* time curves, and the retained product *vs.* time curves indicates that the difference is the higher, the lower the temperature.

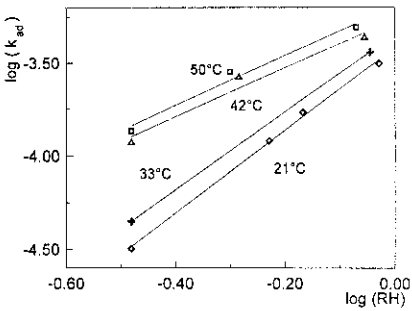

Fig. 8 log-log plots of k_{ads} *vs. RH*

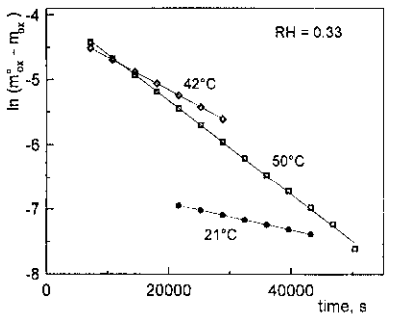

Fig. 9 Plots of experimental data as $\log(m^{\circ}_{ox} - m_{ox})$ *vs.* time

As the m_{ox} *vs.* time curves demonstrate a similar development, the reaction rate may be expressed by the same type of differential equation, namely:

$$\frac{d(m_{ox}/m^{\circ}_{ox})}{dt} = k_{ox}\frac{1 - m_{ox}}{m^{\circ}_{ox}} \tag{3}$$

where m_{ox} is the mass of oxide formed and k_{ox} is the corresponding rate constant. As stated above, m°_{ox} is the value corresponding to the completion of the reaction.

Then, integration yields

$$\frac{m_{ox}}{m^{\circ}_{ox}} = 1 - \exp(-k_{ox}t) \tag{4}$$

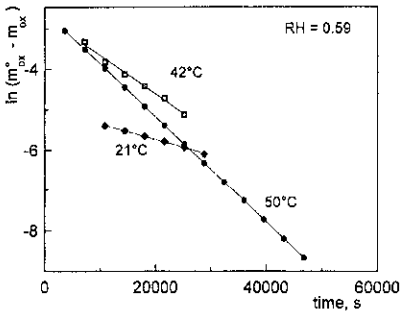

Fig. 10 Plots of experimental data as $\log(m^{\circ}_{ox} - m_{ox})$ *vs.* time

The experimental data fit the resulting equation, as seen in Figs 9 and 10. From the corresponding graphs, the reaction constants were calculated. The values obtained are plotted as a function of *RH* in Fig. 11, from which a dependence on $(RH)^{1.3}$ is obtained. In this case too, the exponent may be related to the number of water molecules reacting on the surface, $(n-1)$ in the reaction scheme.

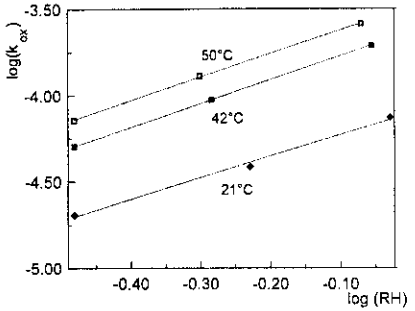

Fig. 11 log-log plots of k_{ox} *vs. RH*

Both rate constants follow an Arrhenius dependence on temperature, as seen in Fig. 12. When the above-mentioned dependence on *RH* is taken into account, the plotted data are k_{ads} and k_{ox} divided by the *RH* value to the corresponding exponent. In this way, activation energy values of 11 kJ mol^{-1} for adsorption and 34 kJ mol^{-1} for reaction were obtained.

In the presence of oxygen

As the experimental curves display a similar development in this case, the kinetic law was expressed, as before, by

$$\frac{d(m_{ox}/m^{\circ}_{ox})}{dt} = k'_{ox}\left(1 - \frac{m_{ox}}{m^{\circ}_{ox}}\right) \tag{5}$$

which, on integration, gives

$$\frac{m_{ox}}{m_{ox}^{0}} = 1 - \exp(-k'_{ox}\, t) \tag{6}$$

where m_{ox} is the mass of oxide formed and k'_{ox} is the corresponding rate constant. As stated above, m_{ox}^{0} is the value corresponding to the completion of the reaction.

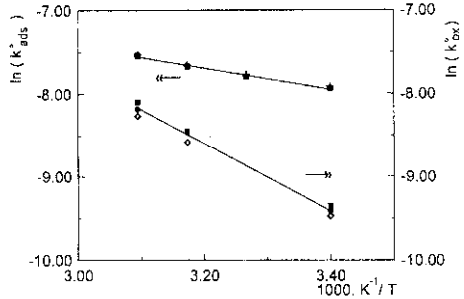

Fig. 12 Arrhenius plots of *RH*-corrected adsorption and reaction rate constants

The experimental data again fit the equation obtained, as seen in Fig. 13. From the corresponding graphs, the reaction constants under different working conditions were calculated. The resulting values are plotted as a function of *RH* in Fig. 14, from which a dependence on $(RH)^{0.8}$ is obtained. In this case too, the exponent may be related to the number of water molecules reacting on the surface. As before, the k'_{ox} data divided by the *RH* value to the corresponding exponent follow an Arrhenius relationship with temperature, as may be seen in Fig. 15. In this way, an activation energy of 21 kJ mol^{-1} for reaction was obtained.

As concerns the different 'orders of reaction' with *RH* for the two cases, they reflect the fact that in the absence of oxygen more water molecules are consumed to form the same product as compared with the process in the presence of oxy-

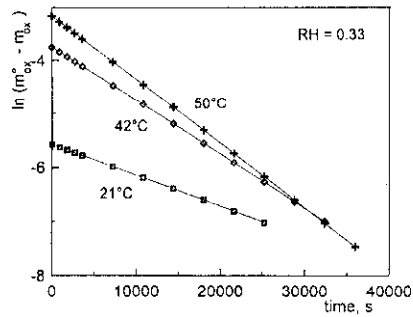

Fig. 13 Plots of experimental data as $\log(m_{ox}^{0} - m_{ox})$ *vs.* time

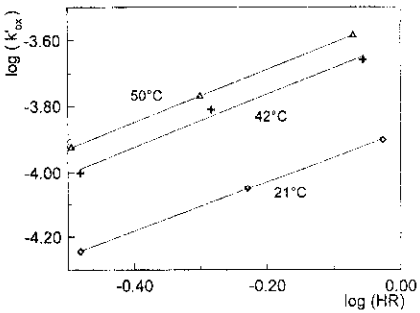

Fig. 14 log-log plots of k_{ox} *vs. RH*

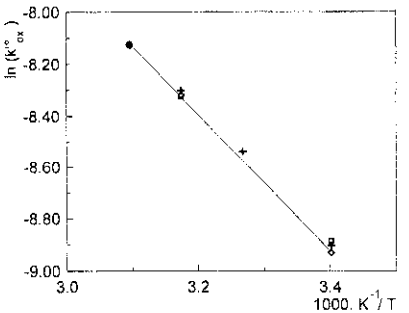

Fig. 15 Arrhenius plots of *RH*-corrected reaction rate constants

gen. Further, with regard to the general concept that apparent activation energies of processes involving pre-equilibrium steps are the sums of actual activation energy plus the corresponding reaction enthalpies, the higher experimental energy of activation for the reaction without oxygen may be explained on the basis of the two previous equilibria postulated in the mechanism as compared to only one for the second case.

* * *

This work was supported by grants from CIC province of Buenos Aires, CONICET, and the Universidad Nacional del Sur, Argentina. J. C. Bazán is a Research Fellow of CIC.

References

1 J. C. Bazán and M. E. G. de Ferreira, Corrosion Sci., 20 (1980) 1129.
2 J. C. Bazán and G. A. Alimenti, Materials Chemistry and Physics, to be published.
3 T. E. Graedel, J. Electrochem. Soc., 136 (1989) 193C.
4 P. W. Winston and D. H. Bates, Ecology, 41 (1960) 232.
5 T. Morimoto and M. Nagao, Bull. Chem. Soc. Japan, 43 (1970) 3746.
6 M. Nagao, J. Phys. Chem., 75 (1971) 3822.
7 Thiel and Madey, Surface Science Reports, 7 (1987) 211.